Biochemistry

 Volume 36, Number 33 August 19, 1997

Accelerated Publications

Structure and Function of the Conserved Domain in αA-Crystallin. Site-Directed Spin Labeling Identifies a β-Strand Located near a Subunit Interface†

Anderee R. Berengian, Michael P. Bova, and Hassane S. Mchaourab*

Biophysics Research Institute, Medical College of Wisconsin, 8701 Watertown Plank Road, Milwaukee, Wisconsin 53226

Received May 27, 1997; Revised Manuscript Received June 27, 1997[⊗]

ABSTRACT: Twelve sequential single cysteine mutants of αA-crystallin extending between amino acids Y109 and L120 were prepared and reacted with a sulfhydryl specific spin label in order to investigate the role of this sequence in the assembly of the αA-crystallin quaternary structure and its chaperone-like function. The sequence is located in the region of highest homology in the α-crystallin domain, a stretch of 100 amino acids conserved among lens α-crystallins and small heat-shock proteins (sHSPs). Analysis of the solvent accessibility and mobility of the attached nitroxides reveals that the sequence, as a whole, is relatively sequestered from the aqueous solvent. Furthermore, as the nitroxide is scanned across the sequence, both mobility and accessibility vary with a periodicity of 2, demonstrating that the backbone conformation is that of a β-strand. One face of the strand, containing the highly conserved residues R112 and R116, is buried with virtually no accessibility to the aqueous solvent. Equivalent strands from different subunits are in close spatial proximity, as inferred from spin−spin interactions between identical residues along the strand. Taken together, our results are consistent with the hypothesis that the α-crystallin domain is a building block of the α-crystallins quaternary structure and suggest that the charge conservation observed in the α-crystallins evolution might be important for the assembly of the oligomer. This work reports the first use of SDSL to identify a β-strand in an unknown structure and demonstrates the feasibility of using this technique to investigate the oligomeric structure of the α-crystallins and sHSPs.

α-Crystallin is one of the major components of the protein matrix in the vertebrate lens and plays an important role in establishing its optical properties (Groenen et al., 1994). In the native state, α-crystallin exists as large homo- or heteromeric complexes, containing about 30−40 subunits, with an apparent molecular mass of 600−900 kDa. These complexes consist of two distinct gene-product subunits, αA and αB, comprising 173 and 175 amino acids, respectively, and sharing extensive sequence homology. Both subunits can exchange between α-crystallin multimers resulting in the observed polydispersed molecular mass of the α-crystallin complexes and their heterogeneity (van den Oetelaar et al., 1990).

Initially considered as a structural protein whose function is to participate in the spatial order of lens proteins, compelling evidence now suggests that α-crystallin is involved in the long-term maintenance of lens transparency. Both α-crystallin subunits share sequence similarity with small heat-shock proteins (sHSPs)[1] from many organisms

† This work was supported by Grants GM22923, EY01931, and RR01008 from the National Institutes of Health.

* Author to whom correspondence should be addressed.

[⊗] Abstract published in *Advance ACS Abstracts,* August 1, 1997.

[1] Abbreviations: Circular dichroism, CD; dithiothreitol, DTT; electron paramagnetic resonance, EPR; Ni(II)ethylenediaminediacetate, NiEDDA; polymerase chain reaction, PCR; site-directed spin labeling, SDSL; small heat-shock proteins, sHSPs; T4 lysozyme, T4L; wild-type, WT.

S0006-2960(97)01234-8 CCC: $14.00

(Caspers et al., 1995). Although the homology is confined to a stretch of 100 residues in the C-terminal domain, termed the α-crystallin domain, α-crystallin subunits and the sHSPs have both a dynamic oligomeric structure and the ability to suppress nonspecific aggregation of proteins (Horwitz, 1992; Merck et al., 1993). This chaperone-like activity is independent of ATP and results in a stable complex between α-crystallin and its protein−substrate (Rao et al., 1993). Consistent with their role as stress proteins, αB and to a lesser extent αA, are expressed in nonlenticular tissues (Bhat & Nagineni, 1989; Kato et al., 1991). The expression of αB is induced in response to thermal stress (Klemenz et al., 1991) while the expression of αA confers thermotolerance (van den Ijssel, 1994). The functional similarity and the common oligomeric structure, coupled to the conservation of the C-terminal domain, led to the hypothesis that the α-crystallins evolved from a single sHSP ancestor (Ingolia & Craig, 1982; de Jong et al., 1993). Therefore, like the other crystallins, their presence in the lens is the result of evolutionary recruitment (Merck et al., 1993; de Jong et al., 1993). Their tendency to form ordered structures contributes to the formation of the transparent lens, while their functional role as heat-shock proteins renders the lens fiber cells stress tolerant (Horwitz, 1992).

The structural equivalent of this hypothesis is that the α-crystallin domain has been recruited as a building block to construct proteins with diverse functions sharing similar structural motifs (Wistow, 1993). Thus, conserved sequences in the α-crystallin domain are expected to form a structural core that plays a central role in the assembly and dynamics of the oligomeric structure and also in the ability of the sHSPs to bind unfolded proteins. Attempts at evaluating this hypothesis have been hampered by the lack of adequate structural tools. Efforts to study the structure of α-crystallin by X-ray crystallography have failed mainly because of the dynamic nature of the aggregate and its microheterogeneity (Groenen et al., 1994). At 800 kDa, α-crystallin is too large for structure determination by nuclear magnetic resonance (NMR). Thus, little is known concerning the tertiary structure of the subunits and their arrangement in the oligomer. A model by Wistow (1985) proposes that the tertiary structure of each subunit consists of two domains, each of two symmetry-related motifs, consisting mainly of β-strands, with a C-terminal extended arm (Wistow, 1985). Evidence in support of the two-domain tertiary structure includes the independent expression of the recombinant C- and N-terminal domains in *Escherichia coli* (Merck et al., 1992) and unfolding experiments consistent with the presence of two independent folding units (Carver et al., 1993). Wistow (1993) also proposed that intersubunit contacts in the C-terminal domain mediate the formation of a basic tetrameric unit that is a building block for the native oligomer (Wistow, 1993). Alternative models for the quaternary structure include a three-layer model (Tardieu et al., 1986), a protein micelle model (Augusteyn & Koretz, 1987), and a cylindrical GroEL-like model (Carver et al., 1994). However, like the model for the tertiary structure, their critical evaluation awaits structural information.

For this purpose, we have initiated a systematic cysteine-scanning mutagenesis and site-directed spin-labeling (SDSL) study of αA-crystallin. Our goals are to study the structure of the subunit at the level of the backbone fold, determine the subunit arrangement and symmetry in the oligomer, and evaluate the role of the α-crystallin domain in conferring common functional and structural features. In cysteine-scanning mutagenesis, a sequential set of mutant proteins is generated and analyzed for structural and functional alterations allowing the evaluation of residues with respect to protein function and molecular interactions. Additionally, the cysteine mutants serve as attachment sites for site-specific incorporation of spin-label probes. Two levels of structural information can be deduced from EPR analysis of the spin-labeled mutants (Hubbell & Altenbach, 1994; Hubbell et al., 1996). The first level consists of the location of the secondary structural elements along the amino acid sequence and their orientation relative to the protein fold. This is deduced from the mobility and solvent accessibility of nitroxide side chains scanned across the sequence (Hubbell et al., 1996). The second level of structural information consists of global geometric constraints that localize the secondary structures or domains relative to each other and is deduced from analysis of distances between pairs of nitroxides (Farrens et al., 1996; Mchaourab et al., 1997). Recently, the feasibility of SDSL in water-soluble proteins has been established (Hubbell et al., 1996).

In the present work, this integrated structural−functional approach is applied to investigate the region between residues 109 and 120 within the α-crystallin domain of αA-crystallin. This region was selected based on the multiple sequence alignment of de Jong and co-workers (1993) showing that the sequence homology between αA and αB exceeds 80% in the region between residues 101 and 120 (Caspers et al., 1995). The results demonstrate the existence of a β-strand along the sequence, identify a subunit interface in αA-crystallin, and provide the first experimental verification that conserved sequences in the α-crystallin domain are involved in the formation of the oligomeric structure. The data is interpreted in terms of the oligomer symmetry and the proposed models of αA-crystallin.

EXPERIMENTAL PROCEDURES

Materials. Spin label I was a generous gift from Professor Kalman Hideg. NiEDDA was kindly provided by Dr. Christian Altenbach. Source Q media, Superose 6, and Hitrap columns were obtained from Pharmacia Biotech. Bovine insulin was from Sigma.

Gene Synthesis and Site-Directed Mutagenesis. The synthetic gene of rat αA-crystallin was constructed as previously described (Dillon & Rosen, 1990) using the nucleotide sequence obtained from GenBank (Accession Number U47922) except that cysteine 131 was replaced with an alanine. Four PCR fragments were ligated. The product was then subcloned into the pET 20b(+) expression vector between the *Nde*I and *Xho*I sites. Because of the high level of expression of recombinant αA (Merck et al., 1992), the nucleotide sequence was only changed to introduce unique restriction sites.

Site-directed mutagenesis was performed using PCR methods as previously described (Mchaourab et al., 1996). For the sequence 109−120, the unique restriction sites *Eco*RV and *Kpn*I were used. Synthetic oligonucleotides, overlapping the *Kpn*I site and containing the point mutation X → cysteine, were used to generate PCR fragments. These fragments were then digested with *Kpn*I and *Eco*RV and subcloned. For all mutant constructs, the entire portion of

the gene amplified was sequenced to confirm the mutation and verify the absence of unwanted changes. Single-site mutants are named by specifying the original residue, the number of the residue, and the new residue, in that order. The αA-crystallin base mutant containing the C131A substitution is referred to as WT*.

Expression and Purification of αA-Crystallin Mutants. Mutant plasmids were used to transform competent *E. coli* BL21(DE3). Cultures, inoculated from overnight seeds, were grown to midlog phase at 37 °C. Then, the synthesis of αA-crystallin was induced by the addition of 0.4 mM IPTG. After 4 h of induction at 30−32 °C, the cells were harvested by centrifugation and resuspended into a lysis buffer containing 20 mM Tris, 1 mM EDTA, 100 mM NaCl, and 10 mM DTT, pH 8. The resuspended cultures were then disrupted by sonication and the DNA precipitated by the addition of 0.06% polyethylenimine. The lysates were then centrifuged at 15000*g* and loaded on a source Q column. After washing with 10 column volumes, αA-crystallin was eluted with a 1 M NaCl gradient. The mutants were further purified by gel filtration on a superose 6 column. Sample purity was analyzed by SDS−PAGE and found to be better than 90%.

Spin Labeling of αA-Crystallin Mutants. Typically, mutant αA-crystallins were incubated in 5-fold molar excess of spin label I to generate side-chain R1 as shown below (Berliner et al., 1982). The reaction was allowed to proceed

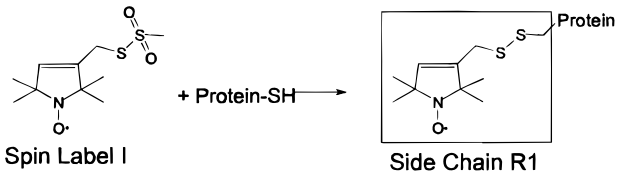

overnight at 4 °C. The samples were then desalted to remove unreacted spin labels using a HiTrap column. The efficiency of labeling was determined by comparing the double integral of the EPR spectrum to that of an 80 μM solution of 4-hydroxy Tempo. Protein concentrations were determined using $\epsilon_{280} = 16\,500\ M^{-1}\ cm^{-1}$ (Horwitz et al., 1997). For all mutants, the labeling efficiency appeared to be ≥85%.

Circular Dichroism. CD analysis was performed on a Jasco 710 spectropolarimeter. Measurements were taken at room temperature in the range 190−260 nm. Protein samples were prepared in 20 mM phosphate, pH 7.1, at a concentration of 0.15 mg/mL.

Chaperone Assays. Aggregation of the insulin B chain was monitored by measuring the apparent absorption due to scattering at 360 nm. Insulin, dissolved into 50 mM sodium phosphate and 100 mM NaCl at a concentration of 0.4 mg/mL, was reduced with 50 mM DTT in the presence of variable amounts of WT or mutant αA-crystallins (Farahbakhsh et al., 1995).

EPR Measurements. EPR spectroscopy was performed on a Varian E102 spectrometer fitted with a two-loop, one-gap resonator. Samples were loaded in gas-permeable TPX capillaries. The microwave power was 2 mW incident, and the modulation amplitude was ≤2 G. The EPR accessibility parameter Π was calculated as previously described (Farahbakhsh et al., 1992) except that changes in $\Delta P_{1/2}$ were normalized to a DPPH powder sample.

Table 1: Average Molecular Mass of R1-Labeled αA-Crystallin Mutants

mutant	average molecular mass (MDa)
WT	0.65
WT*	0.64
Y109R1	0.70
I110R1	0.77
S111R1	0.69
R112R1	0.72
E113R1	0.69
F114R1	0.87
H115R1	0.61
R116R1	0.85
R117R1	0.72
Y118R1	0.65
R119R1	0.56
L120R1	0.59
I110R1 Ex[a]	0.66
S111R1 Ex[a]	0.62
R112R1 Ex[a]	0.63
E113R1 Ex[a]	0.65

[a] In the presence of 4-fold molar excess WT*.

RESULTS

Characterization of the Mutants. The oligomeric structure of the R1-labeled mutants was examined using size-exclusion chromatography. For this purpose, all samples were injected from identical volumes and were chromatographed at the same flow rate on a superose 6 column calibrated using the appropriate molecular mass standards. As shown in Table 1, all R1-labeled mutants assemble into the large molecular mass oligomer. Furthermore, the oligomers do not appear to be in equilibrium with any other species of smaller molecular mass, on the time scale and resolution of the gel filtration experiment. Thus, the introduction of the side chain R1 at these sites did not result in any observable dissociation of the oligomer.

The apparent average molecular mass of the spin-labeled mutants, calculated from their elution volume, is shown in Table 1. Our data show a molecular mass of 640 kDa for the WT and the WT* variant, consistent with previous reports (Smulders et al., 1995a; Horwitz et al., in press). However, the average molecular mass of many mutants is different from that of the WT. Particularly, for the even mutants I110R1, R112R1, F114R1, and R116R1, a significant increase in elution volumes was consistently observed. This may reflect an increase in the number of subunits in the oligomer. For instance, in the case of F114R1, the oligomer appears to consist of 42 subunits as opposed to 32 subunits in the WT. On the other hand, the apparent change in molecular weight can represent changes in the hydrodynamic radius, due to structural rearrangement in subunits or along subunit interfaces, caused by the mutations (Smulders et al., 1995a). The location of the mutated residues near a subunit interface, as revealed by the EPR analysis below, makes this alternative interpretation plausible.

To assess the effects of the mutations on secondary structural content, the R1-labeled mutants were further characterized by far-UV circular dichroism (CD). In Figure 1a, the CD spectrum of the WT* is superimposed on that of the WT, indicating that the global secondary structure of the protein was not affected by the C131A substitution. As shown in Figure 1b, all odd mutants display a CD spectrum characteristic of WT αA-crystallin, with a minimum at 217 nm corresponding to a mainly β-sheet structure. The

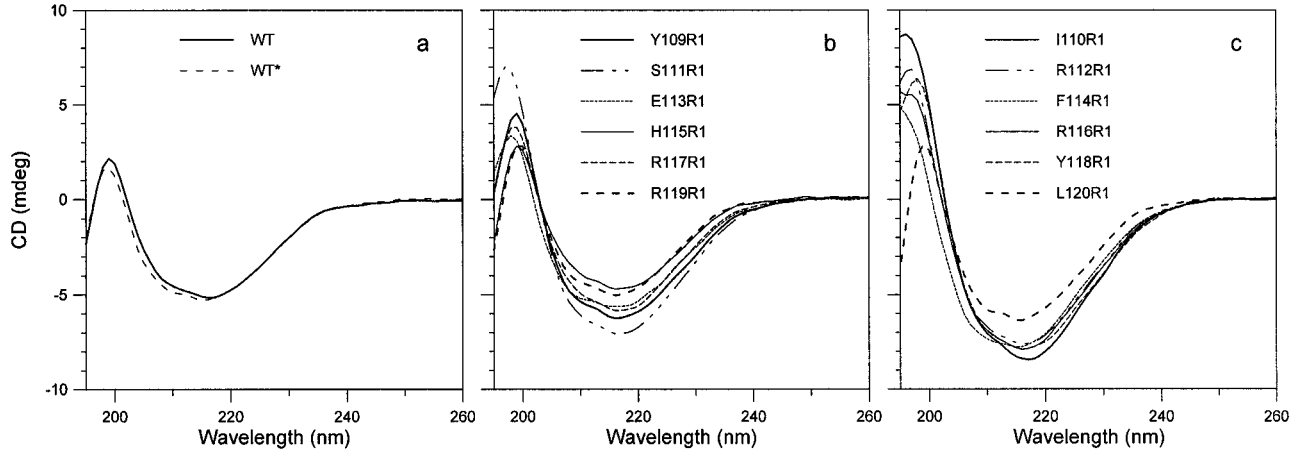

FIGURE 1: Far-UV circular dichroism spectra of αA-crystallin and its mutants. Spectra are the average of 16 scans.

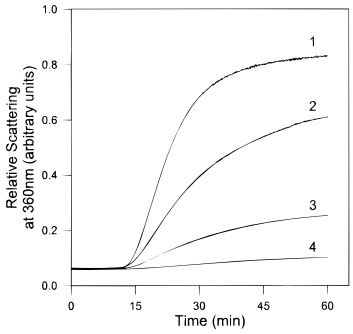

FIGURE 2: Aggregation of the insulin B chain after reduction by dithiothreitol in the absence and presence of αA-crystallin. The insulin to αA-crystallin weight ratios are (1) 1:0, (2) 1:1, (3) 1:3, and (4) 1:5.

variation in ellipticity in the 210−220 nm region is likely the result of errors in the estimation of protein concentration. We found that the ellipticity in this region can vary by as much as 10% for two different preparations of the same mutant. This observation, coupled with the lack of change in the shape of the spectra for most mutants, strongly suggests that mutations at odd sites result in little or no perturbation of the secondary structure.

A similar conclusion can be inferred from the spectra of the even mutants, except F114R1 and R116R1. Figure 1c shows that the CD spectra of the majority of the mutants have a minimum at 217 nm, consistent with a mainly β-sheet conformation. The spectra of F114R1 and R116R1 show distinct changes in the region around 208 nm. Furthermore, all the spectra display changes in the 195−200 nm region. Such changes were previously observed when R1 was introduced at buried and tertiary contact sites in T4 lysozyme (T4L) (Mchaourab et al., 1996). Similar alterations in this spectral region were observed in core mutants of thioredoxin (Wynn & Richards, 1993) and attributed to changes in the packing of secondary structural elements.

The effect of the mutations on the chaperone-like activity was evaluated based on their ability to suppress the aggregation of the insulin B chain. The advantage of the insulin assay is that it is conducted at room temperature where all the mutants are thermodynamically stable. Following reduction of the interchain disulfide bond of insulin, the B chain aggregates resulting in an increase in absorbance at 360 nm as shown in Figure 2, curve 1 (Farahbakhsh et al., 1995). Under our conditions, almost complete suppression of aggregation was obtained with a 1:5 weight ratio of insulin: WT (Figure 2, curve 4). All cysteine mutants are essentially as efficient as the WT in suppressing the aggregation of insulin (not shown). The resulting curves are superimposable on that of the WT for the majority of the mutants. A slight increase in the chaperone-like activity was noted for mutants R112C and F114C.

Side-Chain Mobility along the Sequence. The room-temperature EPR spectra of R1-labeled αA-crystallin mutants are shown in Figure 3. All spectra were normalized to represent the same number of spins. Thus, variation in the spectral intensity between mutants is due predominantly to variation in R1 mobility and/or to spin−spin interaction. Spin−spin interaction between nitroxides separated by ≤15 Å results in a drop in signal intensity and the appearance of spectral intensities extending over more than 100 G (Mchaourab et al., 1997). Such characteristics are observed in the spectra of I110R1, S111R1, R112R1, and E113R1, indicating spin−spin interaction between nitroxides in close proximity (shown by arrows in Figure 3). For this reason, the spectra of R1 at sites I110−E113 are displayed with a 200 G scan width. Since the R1 side chains are on different monomers, the spin−spin interaction must arise from the assembly of the subunits in the oligomer. Almost identical spectra were obtained at sites 110−113 when the labeling was carried out in the unfolded state.

To obtain the mobility and accessibility parameters at these sites, WT* was incubated with each mutant at a molar ratio of 4:1 in the presence of 6 M urea. The mixed protein was then refolded by rapid dilution to a urea concentration of less than 1 M. The refolding pH and ionic strength were similar to those used by de Jong and co-workers (1993). Under these conditions, αA-crystallin refolds reversibly and has similar structural and functional characteristics to lens αA-crystallin (Smulders et al., 1995b). These spin-diluted oligomers were then purified by size-exclusion chromatography. The apparent molecular mass of each oligomer is reported in Table 1. As expected the molecular mass of these predominantly WT* oligomers was similar to WT αA-crystallin. Figure 4 shows the EPR spectra of R1 in the spin-diluted oligomers. The increase in spectral intensity and the disappearance of the spectral features corresponding to the dipolar broadening further support our interpretation that these residues are located near a subunit interface.

In the absence of spin−spin interaction, the EPR spectral line shape reflects the local steric restrictions on the mobility of R1. Spectral line shapes such as those observed at the

FIGURE 3: Room-temperature EPR spectra of the R1-labeled αA-crystallin mutants. Spectra were normalized by double integration to represent the same number of spins. All spectra were recorded with a 100 G scan width except for 110R1, 111R1, 112R1, and 113R1, which have a scan width of 200 G. In several spectra, sharp features seen at the high field resonance position are due to ≤5% unreacted nitroxide spin label in solution.

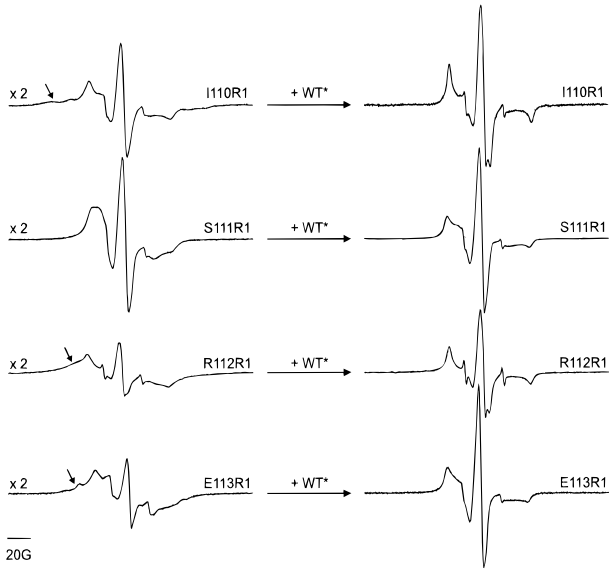

FIGURE 4: Room temperature EPR spectra of the R1-labeled αA-crystallin mutants in the presence of 4-fold molar excess of WT*. All spectra were recorded with a 200 G scan width. They were normalized to represent the same number of spins and scaled for convenience of representation. The scaling factor is shown to the left of each spectrum.

even residues indicate strong steric interaction and are similar to spectra obtained at sites buried in the hydrophobic core of T4L (Mchaourab et al., 1996). The tight packing at these sites allows little motion of the nitroxide relative to the protein matrix on the nanosecond time scale, hence their nearly rigid limit spectra. The spectra at odd sites, on the other hand, are more similar to those obtained at tertiary contact sites in T4L (Mchaourab et al., 1996). Tertiary contact sites are partially buried sites where R1 is in steric contact with proximal side-chain and main-chain atoms. However, unlike buried sites, the distribution of these atoms around the nitroxide moiety is not isotropic, resulting in a relatively less restricted mobility. Tertiary contact sites are spectroscopically distinct in that the spectra of R1 are characterized by the presence of two populations of R1 with different mobilities. Such two-component spectra are observed at all odd sites (Figure 3). In αA-crystallin, steric contacts arise from interaction within the fold of a subunit or from interaction with a neighboring subunit in the oligomeric structure.

As established previously (Mchaourab et al., 1996), the motional information encoded in the spectral line shape can be summarized in a quantitative way using the line width of the central resonance, ΔH_o. Figure 5 shows the values of $(\Delta H_o)^{-1}$ calculated from the spectra of R1 as it is scanned along the 109−120 sequence. The plot clearly reveals a periodic behavior reflecting the presence of two distinct structural environments. The numerical values of $(\Delta H_o)^{-1}$ at the odd residues, except R119R1, are all less than 0.3 G^{-1} similar to those obtained at tertiary contact sites in T4L while those at the even sites are similar to those obtained at buried sites (Mchaourab et al., 1996).

Accessibility Profile of the 109−120 Sequence. Further structural characterization of the sequence can be accomplished by examining the accessibility of the R1 side chain to water-soluble, polar paramagnetic reagents such as NiEDDA. Because of its polarity and size, NiEDDA has hardly any solubility in the buried regions of proteins. Thus, R1 at residues buried in the protein hydrophobic core or along surfaces of subunit contact is expected to have low collision frequencies compared to surface exposed residues. In SDSL, the collision frequency is determined from changes in the saturation parameters of the nitroxide and is expressed through the EPR accessibility parameter Π. That R1 samples two distinct structural environments is further supported by the periodic variation in Π, in the presence of 3 mM NiEDDA, as R1 is scanned across the sequence, shown in Figure 5. The plot reveals a striking oscillatory behavior with a period of 2, indicating that R1 alternates between two environments with different solvent accessibilities. The periodic pattern strongly suggests that the backbone conformation is that of a β-strand (Hubbell et al., 1996). The phase of the period indicates that the even residues, including R112 and R116, form the buried surface of the strand, in agreement with the mobility data. Similar periodicity was observed in the presence of molecular oxygen (Figure 5). Neither mobility nor accessibility was appreciably changed in the pH range 6.9−7.5. They were also independent of protein concentration in the range 4−10 mg/mL.

The absolute values of Π indicate a relatively low solvent accessibility for the sequence as a whole. Comparison of Π values with those obtained in T4L suggests that most residues are either buried or in strong steric contact, except R119R1. The higher accessibility of R119R1 and its relatively higher mobility indicate that this residue is probably on the exposed surface of the oligomer.

DISCUSSION

This paper reports the first nitroxide scanning experiment of αA-crystallin. The sequence between residues Y109 and

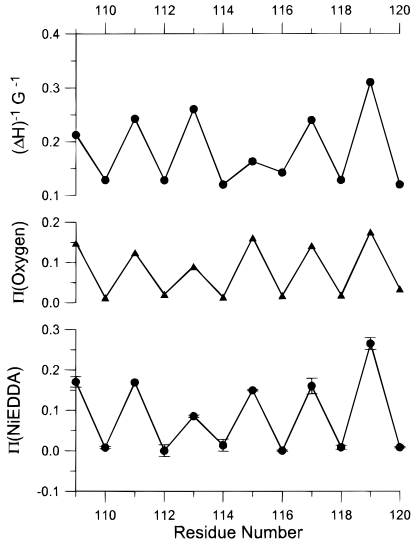

FIGURE 5: Reciprocal of the central line width ΔH^{-1} (●, top), Π (O_2) (▲), and Π (NiEDDA) (●, bottom) versus the residue number.

L120 was selected because it is in a region of high homology among the α-crystallins and appears to be conserved among sHSPs in general (Caspers et al., 1995). The evolutionary profile reveals a familiar characteristic of the α-crystallins, namely the rigid conservation of charged residues, in this case R112 and R116. Furthermore, the sequence is flanked by a glycine (G108) and a proline (P121), suggesting the existence of a regular secondary structural element. In homologous proteins, highly conserved sequences form a common structural core and are involved in packing the hydrophobic core and/or contribute to the interface between subunits (Chothia & Lesk, 1986). The objectives of this work were to (1) evaluate the structural and functional consequences of mutating residues Y109-L120, (2) determine the local conformation and the solvent accessibility profile, and (3) examine whether this sequence is involved in subunit contacts.

Structural and Functional Consequences of the Mutations. Systematic R1 mutagenesis along the 109−120 sequence reveals a binary pattern of perturbation with the R1 substitution at even residues leading to observable changes in the structure but not the chaperone properties of αA-crystallin. At these residues, the changes in the average molecular mass were accompanied by detectable alterations in the CD spectrum, particularly in the 195−200 nm region. Of notable significance is the changes in the average molecular mass and far UV-CD associated with the R116R1 substitution. In oligomeric proteins, subunit interfaces tend to contain charged groups, especially arginines, that are normally involved in salt bridges and/or hydrogen bonds (Janin et al., 1988). The change in stability observed for R116R1 is consistent with the disruption of a buried salt bridge, thus burying a charge in a low dielectric medium. In this context, the observed increase in the average molecular mass most likely reflects structural rearrangements caused by the mutations rather than an increase in the number of subunits in the aggregate. Not only do these mutations disrupt the interactions of the native residues but they should also cause limited repacking at buried sites to accommodate the increased molar volume of R1 (Mchaourab et al., 1996).

Despite their buried locations, the even mutants are as efficient as the WT in suppressing the aggregation of the insulin B chain. Because this assay is conducted under conditions where the global structure of each mutants is intact, only structural alterations in the substrate binding region are likely to affect the binding affinity. It has been proposed that the exposed hydrophobic surfaces of α-crystallin are the substrate binding domain. Given the relatively solvent-inaccessible profile of the sequence, it is unlikely that these residues are involved in protein−substrate binding.

Structure along the Sequence 109−120. As a whole the sequence appears to be sequestered from the solvent as nitroxide side chains have relatively low collision frequency with NiEDDA across the sequence. The data indicate that both odd and even residues are involved in steric contacts with the protein fold. The more extensive interaction at the even residues can be unequivocally identified from their rigid limit EPR spectra and the almost complete absence of collision with either molecular oxygen or NiEDDA. This is consistent with the observed structural destabilization at these sites, usually associated with substitution at residues buried in the hydrophobic core of proteins (Matthews, 1996). Although the odd residues appear to have relatively higher accessibility to NiEDDA, the absolute values of Π, except for R119R1, are lower than that expected for residues exposed on the surface of a β-strand (Hubbell et al., 1996). Thus, these residues have some level of steric interaction presumably with main-chain and side-chain atoms contributed by nearby subunits in the quaternary structure. For each residue, a structural parameter was derived from the analysis of the solvent accessibility of R1 and its mobility. The periodic variation in both parameters across the sequence demonstrates that the nitroxide samples two distinct structural environments. Therefore, we deduce that the backbone conformation along that sequence is that of a β-strand.

Residues I110− E113 Are Involved in Intersubunit Contacts. Our data clearly indicate that equivalent strands, from different subunits, are in spatial proximity in the native oligomer. This is inferred from the extensive broadening of the spectral line shape and the appearance of distinct spectral features resulting from dipolar splitting in the spectra of I110R1−E113R1. Because the tumbling of the interspin vector is slow on the EPR time scale, the observed interaction arises predominantly from static dipole−dipole interaction. The dipolar broadening is determined by the geometry relating the interacting spins and their separation (Hustedt et al., 1997). It is also dependent to a large extent on the conformational heterogeneity of the oligomer. Therefore, we did not quantitatively analyze the separation between R1 side chains at these sites, although the extensive broadening at site R112 indicates a distance of less than 15 Å. The analysis of Figure 4 is sufficient for the purpose of establishing spatial proximities. In this context, the close proximity between E113R1 from different subunits is consistent with the report that mouse HSP25 contains intersubunit disulfide bonds between cysteines present at the equivalent position of E113 in the sequence alignment (Dudich et al., 1995).

Wistow (1993) proposed, and this study confirms, that subunit contacts in the α-crystallin domain are critical for the assembly of the oligomer (Wistow, 1993). In Wistow's model, two different sets of interactions exist: (1) heterologous interactions resulting in the formation of a basic tetrameric building block with 4-fold symmetry and (2) isologous interaction between tetramers resulting in the formation of a rhombic dodechedron oligomer. Because

extensive spin−spin interaction between R1 at equivalent residues implies specific elements of symmetry, in the context of Wistow's model, the segment between I110 and H115 may be involved in contacts between tetramers. Experiments are currently underway to test this hypothesis. Examples of interactions between equivalent strands in oligomeric proteins include hydrogen bonding between two equivalent strands in an antiparallel fashion or the opposition of the equivalent strands at right angle.

Conclusion. The major conclusion of this paper is that one highly conserved sequence, in the α-crystallin domain, is critical for the assembly and stability of αA-crystallin. Conserved charged residues along the sequence are in a buried environment, indicating the presence of buried salt bridges in the core of the oligomer and/or the subunits. A β-strand spans this sequence and is involved in subunit contacts. That this sequence is conserved across sHSPs suggests that the subunit interface is critical for the assembly of the oligomeric structure in this family of proteins.

The results also demonstrate the efficacy of using SDSL to determine the location of β-strands along the sequence of sHSPs. Spin−spin interactions can be used to provide structural constraints on the symmetry of the subunits in the oligomer. With a sufficiently large number of mutants, it should be possible to critically evaluate models of α-crystallins and sHSPs quaternary structure.

ACKNOWLEDGMENT

The authors thank Prof. Joseph Horwitz for helpful suggestions and discussions.

REFERENCES

Augusteyn, R. C., & Koretz, J. F. (1987) *FEBS Lett. 222*, 1−5.
Berliner, L. J., Hankovsky, H. O., & Hideg, K. (1982) *Anal. Biochem. 119*, 450−453.
Bhat, S. P., & Nagineni, C. N. (1989) *Biochem. Biophys. Res. Commun. 158*, 319−325.
Carver, J. A., Aquilina, J. A., & Truscott, R. J. (1993) *Biochim. Biophys. Acta 1164*, 22−28.
Carver, J. A., Aquilina, J. A., & Truscott, R. J. (1994) *Exp. Eye Res. 59*, 231−234.
Caspers, G., Leunissen, J. A. M., & de Jong, W. W. (1995) *J. Mol. Evol. 40*, 238−248.
Chothia, C., & Lesk, A. M. (1986) *EMBO J. 5*, 823−826.
de Jong, W. W., Leunissen, J. A. M., & Voorter, C. E. M. (1993) *Mol. Biol. Evol. 10*, 103−126.
Dillon, P. J., & Rosen, C. A. (1990) *BioTechniques 9*, 298−300.
Dudich, I. V., Zav'yalov, V. P., Pfeil, W., Gaestel, M., Zav'yalova, G. A., Denesyuk, A. I., & Korpela, T. (1995) *Biochim. Biophys. Acta 1253*, 163−168.
Farahbakhsh, Z. T., Altenbach, C., & Hubbell, W. L. (1992) *Photochem. Photobiol. 56*, 1019−1033.
Farahbakhsh, Z. T., Huang, Q., Ding, L., Altenbach, C., Steinhoff, H., Horwitz, J., & Hubbell, W. L. (1995) *Biochemistry 34*, 509−516.
Farrens, D. L., Altenbach, C., Hubbell, W. L., & Khorana, H. G. (1996) *Science 274*, 768−770.
Groenen, P. J. A., Merck, K., de Jong, W. W., & Bloemendal, H. (1994) *Eur. J. Biochem. 225*, 1−19.
Horwitz, J. (1992) *Proc. Natl. Acad. Sci. U.S.A. 89*, 10449−10453.
Horwitz, J., Huang, Q., Ding, L., & Bova, M. P. (1997) *Methods Enzymol.* (in press).
Hubbell, W. L., & Altenbach, C. (1994) *Curr. Opin. Struct. Biol. 4*, 566−573.
Hubbell, W. L., Mchaourab, H. S., Altenbach, C., & Lietzow, M. A. (1996) *Structure 4*, 779−783.
Hustedt, E. J., Smirnov, A. I., Laub, C., Cobb, C. E., & Beth, A. H. (1997) *Biophys. J.* 72, 1861−1877.
Ingolia, T. D., & Craig, E. A. (1982) *Proc. Natl. Acad. Sci. U.S.A. 79*, 2360−2364.
Janin, J., Miller, S., & Chothia, C. (1988) *J. Mol. Biol. 204*, 155−164.
Kato, K., Shinohara, H., Kurobe, N., Goto, S., Inaguma, Y., & Ohshima, K. (1991) *Biochim. Biophys. Acta 1080*, 173−180.
Klemenz, R., Fröhli, E., Steiger, R. H., Schäfer, R., & Aoyama, A. (1991) *Proc. Natl. Acad. Sci. U.S.A. 88*, 3652−3656.
Matthews, B. W. (1995) *Adv. Protein Chem. 46*, 249−278.
Mchaourab, H. S., Lietzow, M. A., Hideg, K., & Hubbell, W. L. (1996) *Biochemistry 35*, 7692−7704.
Mchaourab, H. S., Oh, K. J., Fang, C. J., & Hubbell, W. L. (1997) *Biochemistry 36*, 307−316.
Merck, K. B., de Haard-Hoekman, W. A., Oude Essink, B. B., Bloemendal, H., & de Jong, W. W. (1992) *Biochim. Biophys. Acta 1130*, 267−276.
Merck, K. B., Groenen, P. J. T. A., Voorter, C. E. M., de Haard-Hoekman, W. A., Horwitz, J., Bloemendal, H., & de Jong, W. W. (1993) *J. Biol. Chem. 268*, 1046−1052.
Rao, P. V., Horwitz, J., & Zigler, J. S., Jr. (1993) *Biochem. Biophys. Res. Commun. 190*, 786−793.
Smulders, R. H. P. H., Merck, K. B., Aendekerk, J., Horwitz, J., Takemoto, L., Slingsby, C., Bloemendal, H., & de Jong, W. W. (1995a) *Eur. J. Biochem. 232*, 834−838.
Smulders, R. H. P. H., Van Geel, I. G., Bloemendal, H., & de Jong, W. W. (1995b) *J. Biol. Chem. 270*, 13916−13924.
Tardieu, A., Laporte, D., Licinio, P., Krop, B., & Delaye, M. (1986) *J. Mol. Biol. 192*, 711−724.
van den Ijssel, P., Overkamp, P., Knauf, U., Gaestel, M., & de Jong, W. W. (1994) *FEBS Lett. 355*, 54−56.
van den Oetelaar, P. J. M., Van Someren, P. F. M. H., Thomson, J. A., Siezen, R. J., & Hoenders, H. J. (1990) *Biochemistry 29*, 3488−3493.
Wistow, G. (1985) *FEBS Lett. 181*, 1−6.
Wistow, G. (1993) *Exp. Eye Res. 56*, 729−732.
Wynn, R., & Richards, F. M. (1993) *Protein Sci. 2*, 395−403.

BI9712347